Water-Soluble Graphene Covalently Functionalized by Biocompatible Poly-L-lysine

ARTICLE *in* LANGMUIR · SEPTEMBER 2009

Impact Factor: 4.46 · DOI: 10.1021/la903265p · Source: PubMed

6 AUTHORS, INCLUDING:

Ari Ivaska
Åbo Akademi University
319 PUBLICATIONS **9,576** CITATIONS
SEE PROFILE

Li Niu
Chinese Academy of Sciences
215 PUBLICATIONS **7,047** CITATIONS
SEE PROFILE

Langmuir
Letter

pubs.acs.org/Langmuir

Water-Soluble Graphene Covalently Functionalized by Biocompatible Poly-L-lysine

Changsheng Shan,[†] Huafeng Yang,[†] Dongxue Han,[†,‡] Qixian Zhang,[†] Ari Ivaska,[‡] and Li Niu*[,†,‡]

[†]*State Key Laboratory of Electroanalytical Chemistry, Changchun Institute of Applied Chemistry, and Graduate University of the Chinese Academy of Sciences, Chinese Academy of Sciences, Changchun 130022, P. R. China, and* [‡]*Laboratory of Analytical Chemistry, Process Chemistry Centre, Åbo Akademi University, Åbo-Turku, FI-20500, Finland*

Received August 31, 2009. Revised Manuscript Received September 13, 2009

Graphene sheets functionalized covalently with biocompatible poly-L-lysine (PLL) were first synthesized in an alkaline solution. PLL-functionalized graphene is water-soluble and biocompatible, which makes it a novel material promising for biological applications. Graphene sheets played an important role as connectors to assemble these active amino groups of poly-L-lysine, which provided a very biocompatible environment for further functionalization, such as attaching bioactive molecules. As an example, an amplified biosensor toward H_2O_2 based on linking peroxidase onto PLL-functionalized graphene was investigated.

Introduction

Graphene, which has been considered a "rising star" material, has attracted considerable attention from both the experimental and theoretical scientific communities.[1,2] Because of their novel properties,[3,4] such as exceptional thermal and mechanical properties, high electrical conductivity, graphene sheets have been extensively studied in synthesizing nanocomposites[5−8] and fabricating various microelectrical devices, such as battery,[9] field-effect transistors,[10] ultrasensitive sensors,[11] and electromechanical resonators.[12] Recently, the biological applications of graphene have also started to be concerned.[13−18] For example, Berry et al. fabricated a novel graphene-based live-bacterial-hybrid device and a DNA-hybridization device with excellent sensitivity.[13] Dai et al. synthesized nanoscale graphene oxide sheets by branched polyethylene glycol (PEG) and exhibited the unique ability of graphene in the attachment and delivery of aromatic, water insoluble drugs.[14] Li and Wallace et al. have presented the growth of mouse fibroblast cell (L-929) on graphene paper, which indicated that the graphene paper was biocompatible and suitable for biomedical applications.[16] Fan et al. reported that graphene oxide could facilitate electron transfer of metalloprotein at electrode surface.[18] It is well-known that graphene sheets, which have a high specific surface area, unless well separated from each other, tend to form irreversible agglomerates or even restack to form graphite through strong $\pi-\pi$ stacking and van der Waals interaction.[2] The prevention of aggregation is of particular importance for graphene sheets because most of their unique properties are only associated with individual sheets. Some methods containing covalent and noncovalent functionalization of graphene have been used for obtaining dispersed graphene.[19−22]

To extend the application of graphene, here we reported another convenient method to prepare water-soluble graphene sheets functionalized by biocompatible poly-L-lysine (PLL; the molecular structure is shown in Scheme 1) as a linker through a covalent amide group. PLL has plentiful active amino groups and is useful in promoting cell adhesion and drug delivery. Many kinds of PLL-functionalized nanomaterials have been applied in many fields,[23−27] such as cell labeling, biofuel cells, and DNA electrochemical sensors. PLL has several advantages, such as good biocompatibility, plentiful active amino groups, a flexible

*Corresponding author. Fax: +86-431-8526 2800. E-mail: lniu@ciac.jl.cn.

(1) Geim, A. K.; Novoselov, K. S. *Nat. Mater.* **2007**, *6*, 183–191.
(2) Li, D.; Muller, M. B.; Gilje, S.; Kaner, R. B.; Wallace, G. G. *Nat. Nanotechnol.* **2008**, *3*, 101–105.
(3) Zhang, Y. B.; Tan, Y. W.; Stormer, H. L.; Kim, P. *Nature* **2005**, *438*, 201–204.
(4) Li, X. L.; Zhang, G. Y.; Bai, X. D.; Sun, X. M.; Wang, X. R.; Wang, E.; Dai, H. J. *Nat. Nanotechnol.* **2008**, *3*, 538–542.
(5) Stankovich, S.; Dikin, D. A.; Dommett, G. H. B.; Kohlhaas, K. M.; Zimney, E. J.; Stach, E. A.; Piner, R. D.; Nguyen, S. T.; Ruoff, R. S. *Nature* **2006**, *442*, 282–286.
(6) Xu, Y. X.; Bai, H.; Lu, G. W.; Li, C.; Shi, G. Q. *J. Am. Chem. Soc.* **2008**, *130*, 5856–5867.
(7) Muszynski, R.; Seger, B.; Kamat, P. V. *J. Phys. Chem. C* **2008**, *112*, 5263–5266.
(8) Williarris, G.; Seger, B.; Kamat, P. V. *ACS Nano* **2008**, *2*, 1487–1491.
(9) Cassagneau, T.; Fendler, J. H. *Adv. Mater.* **1998**, *10*, 877–881.
(10) Gilje, S.; Han, S.; Wang, M.; Wang, K. L.; Kaner, R. B. *Nano Lett.* **2007**, *7*, 3394–3398.
(11) Schedin, F.; Geim, A. K.; Morozov, S. V.; Hill, E. W.; Blake, P.; Katsnelson, M. I.; Novoselov, K. S. *Nat. Mater.* **2007**, *6*, 652–655.
(12) Bunch, J. S.; van der Zande, A. M.; Verbridge, S. S.; Frank, I. W.; Tanenbaum, D. M.; Parpia, J. M.; Craighead, H. G.; McEuen, P. L. *Science* **2007**, *315*, 490–493.
(13) Mohanty, N.; Berry, V. *Nano Lett.* **2008**, *8*, 4469–4476.
(14) Liu, Z.; Robinson, J. T.; Sun, X. M.; Dai, H. J. *J. Am. Chem. Soc.* **2008**, *130*, 10876–10877.
(15) Shang, N. G.; Papakonstantinou, P.; McMullan, M.; Chu, M.; Stamboulis, A.; Potenza, A.; Dhesi, S. S.; Marchetto, H. *Adv. Funct. Mater.* **2008**, *18*, 3506–3514.
(16) Chen, H.; Muller, M. B.; Gilmore, K. J.; Wallace, G. G.; Li, D. *Adv. Mater.* **2008**, *20*, 3557–3561.
(17) Shan, C. S.; Yang, H. F.; Song, J. F.; Han, D. X.; Ivaska, A.; Niu, L. *Anal. Chem.* **2009**, *81*, 2378–2382.
(18) Zuo, X. L.; He S. J.; Li D.; Peng C.; Huang Q.; Song S. P.; Fan C. H. *Langmuir* [Early online access].DOI: 10.1021/la902496u. Published online: Aug 20, 2009.
(19) Niyogi, S.; Bekyarova, E.; Itkis, M. E.; McWilliams, J. L.; Hamon, M. A.; Haddon, R. C. *J. Am. Chem. Soc.* **2006**, *128*, 7720–7721.
(20) Si, Y.; Samulski, E. T. *Nano Lett.* **2008**, *8*, 1679–1682.
(21) Shen, J. F.; Hu, Y. H.; Li, C.; Qin, C.; Ye, M. X. *Small* **2009**, *5*, 82–85.
(22) Lomeda, J. R.; Doyle, C. D.; Kosynkin, D. V.; Hwang, W. F.; Tour, J. M. *J. Am. Chem. Soc.* **2008**, *130*, 16201–16206.
(23) Kim, J. B.; Premkumar, T.; Giani, O.; Robin, J. J.; Schue, F.; Geckeler, K. E. *Macromol. Rapid Commun.* **2007**, *28*, 767–771.
(24) Babic, M.; Horak, D.; Trchova, M.; Jendelova, P.; Glogarova, K.; Lesny, P.; Herynek, V.; Hajek, M.; Sykova, E. *Bioconjugate Chem.* **2008**, *19*, 740–750.
(25) Deng, L.; Shang, L.; Wang, Y. Z.; Wang, T.; Chen, H. J.; Dong, S. J. *Electrochem. Commun.* **2008**, *10*, 1012–1015.
(26) Zhang, Y. J.; Li, J.; Shen, Y. F.; Wang, M. J.; Li, J. H. *J. Phys. Chem. B* **2004**, *108*, 15343–15346.
(27) Jiang, C.; Yang, T.; Jiao, K.; Gao, H. W. *Electrochim. Acta* **2008**, *53*, 2917–2924.

Scheme 1. Schematic Diagram of Graphene-PLL Synthesis and Assembly Process of Graphene-PLL and HRP at a Gold Electrode

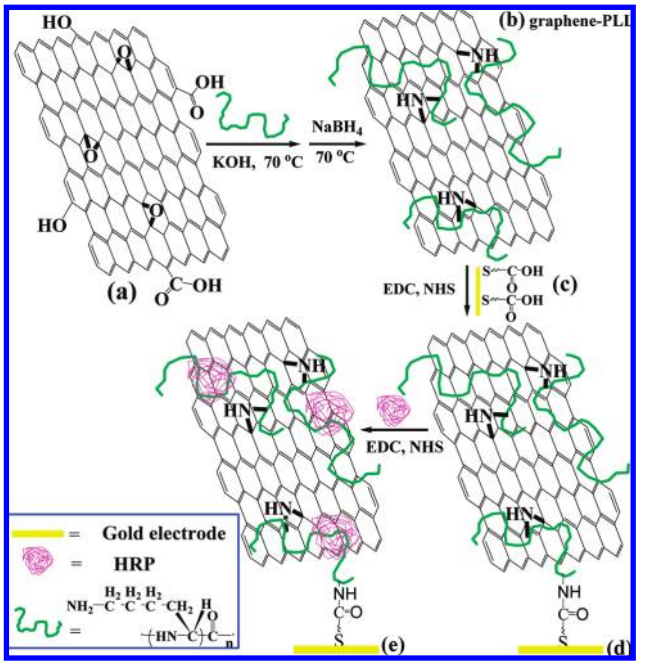

molecular backbone, and relatively good solubility in water. Because of the plentiful epoxy groups of graphene oxides,[28] some free amino groups on the PLL molecular chains cross-linked with those epoxy groups and other residual amino groups acted as a relative "friendly" and "soft" linker between the graphene sheet and bioactive molecules. Therefore, the PLL-functionalized graphene (graphene-PLL) sheets with plentiful amino groups may open a way to a large number of opportunities, such as cell labeling, bioactive molecular attachment, and the preparation of nanocomposites. As a potential application, by further linking peroxidase, an amplified biosensing toward H_2O_2 at such graphene-PLL assembly was investigated.

Experimental Section

Materials. Graphite, hydrazine solution (50 wt %), and ammonia solution (28 wt %) were purchased from Sinopharm Chemical Reagent Co., Ltd. Poly-L-lysine hydrobromide (PLL, M_w = 30000−70000), 3-mercaptopropionic acid (MPA, >99%) and horseradish peroxidase (HRP, 250−330 units/mg) were obtained from Sigma. 1-Ethyl-3(3-dimethylaminopropyl) carbodiimide hydrochloride (EDC) was obtained from Alfa Aesar. *N*-Hydroxysulfosuccinimide sodium (NHS) was obtained from Acros organics. Hydrogen peroxide solution (30 wt %) was purchased from Beijing Chemical Reagent (Beijing, China), and a fresh solution of H_2O_2 was prepared daily. All other reagents were of analytical grade and were used as received. Aqueous solutions were prepared with double-distilled water from a Millipore system (>18 MΩ cm).

Instruments. Ultraviolet−visible (UV−vis) absorption spectra of graphene-PLL aqueous solution were collected using a CARY 500 Scan UV/vis/NIR spectrophotometer. Fourier transform infrared spectroscopy (FTIR) was recorded on a Bruker Vertex 70 spectrometer (4 cm^{-1}). Tapping-mode Atomic force microscopy (AFM) imaging was performed on a Digital Instruments multimode microscope controlled by Nanoscope IIIa apparatus (Digital Instruments, Santa Barbara, CA) equipped with a J scanner. X-ray photoelectron spectroscopy (XPS) analysis was carried out on an ESCALAB MK II X-ray photoelectron spectrometer. Energy dispersive X-ray spectroscopy (EDX) was measured on a 2000XMS Instrument (EDAX, Inc.). Cyclic voltammetric (CV) measurements were performed using a conventional three-electrode cell with a platinum wire as the auxiliary electrode and Ag|AgCl (saturated KCl) as the reference in a CHI 660 Electrochemical Workstation (CHI, USA). Working electrodes were modified gold electrodes (d = 2 mm). Before use, gold electrodes were carefully polished to a mirror finish with 1.0-, 0.3-, and 0.05-μm alumina slurries, successively.

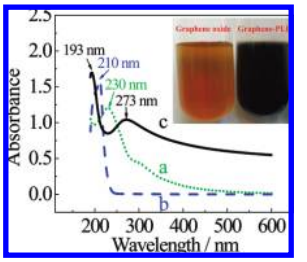

Figure 1. UV−vis spectra of graphene oxides (a), PLL (b), and graphene-PLL nanocomposites (c). The inset: photo of graphene oxides and graphene-PLL aqueous solution.

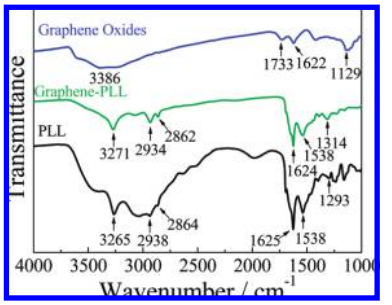

Figure 2. FTIR spectra of graphene oxides (blue), graphene-PLL (green), and PLL (black).

Synthesis of PLL-Functionalized Graphene. Graphite oxides (Scheme 1a) were synthesized from graphite powder by a modified Hummers method.[29,30] Generally, the graphene-PLL (as shown in Scheme 1b) was prepared by vigorously stirring a solution of 2 mg of the graphene oxides, 8 mg of PLL, and 10 mg of KOH in 10 mL of H_2O at 70 °C for 24 h. Then 1 mL of 1 M $NaBH_4$ solution was added, and the reaction was kept on at 70 °C for 2 h. After that, the graphene-PLL was collected and purified by centrifugation and adequately washed with water several times to remove the impurities and the excess of PLL by physical absorption.

Preparation of Graphene-PLL/HRP Modified Gold Electrode. As an example, this graphene-PLL assembly was successfully further conjugated with HRP and used to construct a chemically modified gold electrode toward biosensing of H_2O_2. The process of the preparation of a graphene-PLL-modified gold electrode is illustrated in Scheme 1c−e. First, the cleaned gold electrode was immersed in a 0.02 M MPA aqueous solution for 24 h at room temperature (Scheme 1c). Then, it was immersed in 0.05 M PBS buffer (pH 7.4) containing graphene-PLL (0.5 mg/mL), EDC (10 mM), and NHS (5 mM) for 48 h. After that, the Au/MPA/graphene-PLL electrode (Scheme 1d) was immersed in 0.05 M PBS buffer containing HRP (2 mg/mL), EDC (10 mM), and NHS (5 mM) at 4 °C for 24 h to obtain an Au/MPA/Graphene-PLL/HRP composite electrode (Scheme 1e). In each step of the assembly, the electrode was thoroughly rinsed with distilled water to remove

(28) Szabo, T.; Berkesi, O.; Forgo, P.; Josepovits, K.; Sanakis, Y.; Petridis, D.; Dekany, I. *Chem. Mater.* **2006**, *18*, 2740–2749.
(29) Hummers, W. S.; Offeman, R. E. *J. Am. Chem. Soc.* **1958**, *80*, 1339.
(30) Kovtyukhova, N. I.; Ollivier, P. J.; Martin, B. R.; Mallouk, T. E.; Chizhik, S. A.; Buzaneva, E. V.; Gorchinskiy, A. D. *Chem. Mater.* **1999**, *11*, 771–778.

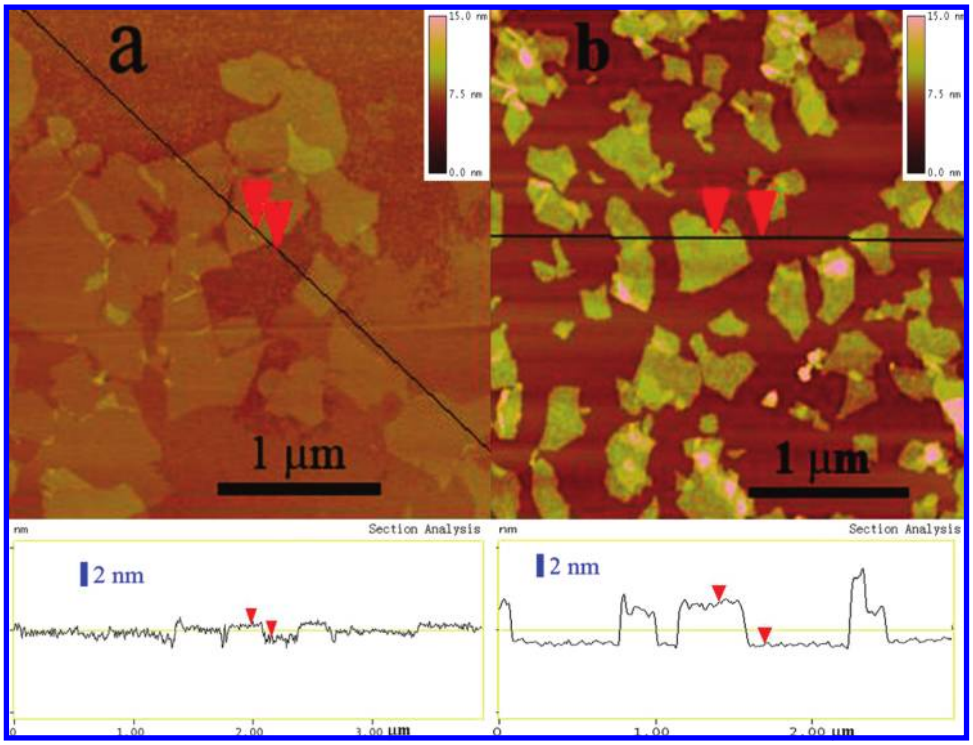

Figure 3. AFM images of graphene oxides (a) and graphene-PLL (b).

the excess of the physical adsorption. The reference Au/MPA/PLL/HRP electrode without graphene was prepared in the same way, except that PLL was used instead of graphene-PLL.

Results and Discussion

A schematic representation of the formation of PLL-functionalized graphene is shown in Scheme 1a,b. The PLL was covalently grafted to graphene through the reaction of epoxy groups on graphene oxides[28] and amino groups on PLL in the presence of KOH.

The formation of graphene-PLL and reduction of graphene oxides are first confirmed by UV−vis spectroscopy. The UV−vis spectra of graphene oxides (Figure 1a) and PLL (Figure 1b) in water show absorption peaks at 230 and 210 nm, respectively. After the formation of graphene-PLL, the absorptions of water-soluble graphene-PLL (Figure 1c) are shifted to 273 and 193 nm, respectively. The absorption of graphene-PLL redshifts from 230 to 273 nm, suggesting that the electronic conjugation within graphene sheets is restored after the reaction.[2] The peak of graphene-PLL at 193 nm is shifted to much shorter wavelengths (210 nm of PLL) due to the interaction of graphene and PLL.[23] The reduction of graphene oxides is also indicated from the color change of solution before and after reaction (from brown to dark, as shown in the inset in Figure 1). At concentrations of 0.5 mg/mL, the resulting graphene-PLL aqueous solution is very stable, even for several months storage without precipitate, which is very favorable for the further applications of this functionalized graphene.

Graphene grafted covalently by PLL can be confirmed by FTIR (Figure 2). The spectrum of graphite oxides showed the presence of O−H (ν_{O-H} at 3386 cm^{-1}), C═O ($\nu_{C=O}$ at 1733 cm^{-1} in carbonyl groups), C═C ($\nu_{C=C}$ at 1622 cm^{-1}), and C−O (ν_{C-O} at 1129 cm^{-1}). After the reduction, the disappearance of characteristic peaks of oxide groups in graphene-PLL indicates that such graphene oxides have been fully reduced to the graphene. The FTIR spectrum of graphene-PLL exhibits PLL absorption features, such as N−H (ν_{N-H} at 3271 cm^{-1} in free NH_3^+ groups), C═O ($\nu_{C=O}$ at 1624 cm^{-1}). Especially, the peak of the C−N stretch mode in graphene-PLL appeared at 1314 cm^{-1} (ν_{C-N} binding with Aromatic Ring). These results confirm that the PLL has been covalently grafted to the graphene sheet successfully. It is noted that the presence of free NH_3^+ groups is very useful for the further functionalization and application of such graphene-PLL nanocomposites.

The formation of graphene and the functionalization of PLL have also been confirmed further by XPS (Figure S1, Supporting Information), which is an effective tool to characterize the removal of the oxygen groups.[31,32] The C1s XPS spectrum of graphene-PLL shows a significant decrease of signals at ca. 286.7 and 288.4 eV, which indicates a loss of C−O and C═O functionalities (Figure S1). Moreover, there are two additional absorbance peaks that appear at 285.4 and 287.6 eV corresponding to the carbon in the C−NH_2 and C−N bonds, respectively.[33] These results suggest that the graphene has been functionalized well by PLL with free NH_2 groups. In addition, the molar ratio of O to C decreases from 0.374 of graphene oxides to 0.156 of graphene-PLL, and nitrogen is present (10.93 at%) in the graphene-PLL characterized by EDX (as shown in Figure S2). These results also suggest that graphene oxides have been reduced totally into graphene during the functionalization by PLL.

AFM images confirm that evaporated dispersions of graphene oxides and graphene-PLL are composed of isolated graphitic sheets (Figure 3). The graphene oxides have lateral dimensions of several hundred nanometers and a thickness of 1 nm (as shown in Figure 3a), which is characteristic of fully exfoliated graphene oxide sheets. After the final reduction step, the mean thickness

(31) Stankovich, S.; Piner, R. D.; Chen, X. Q.; Wu, N. Q.; Nguyen, S. T.; Ruoff, R. S. *J. Mater. Chem.* **2006**, *16*, 155–158.
(32) McAllister, M. J.; Li, J. L.; Adamson, D. H.; Schniepp, H. C.; Abdala, A. A.; Liu, J.; Herrera-Alonso, M.; Milius, D. L.; Car, R.; Prud'homme, R. K.; Aksay, I. A. *Chem. Mater.* **2007**, *19*, 4396–4404.
(33) Everhart, D. S.; Reilley, C. N. *Anal. Chem.* **1981**, *53*, 665–676.

of graphene-PLL was ca. 3.6 nm (Figure 3b). The increase of graphene-PLL in thickness originates from the coverage of PLL on both sides of graphene, which also suggests the formation of PLL-functionalized graphene.

As an example of such graphene-PLL assembly in potential bioassay, the biosensor based on graphene-PLL and HRP assembly was constructed for biosensing H_2O_2. Figure 4 shows the cyclic voltammograms of different modified electrodes in the presence of H_2O_2. The successful modification of HRP on the Au/MPA/graphene-PLL/HRP electrode and the larger loading of HRP compared to the Au/MPA/PLL/HRP electrode were confirmed by CV measurements, as shown in Figure 4. From the distinctive reductive current difference between curves *a* and *c* in Figure 4, it could be inferred that the catalysis toward H_2O_2 reduction at Au/MPA/graphene-PLL/HRP was mainly ascribed to the addition of HRP. The reduction current at Au/MPA/graphene-PLL/HRP (curve *a*) was much larger than that at Au/MPA/PLL/HRP (curve *b*) in this case (2.7-fold greater at −0.3 V), indicating that the larger HRP loading achieved after the introduction of PLL-functionalized graphene due to a large quantity of free amino groups on the electrode substrate. In addition, the onset potential of reduction at Au/MPA/graphene-PLL/HRP (curve *a*) was more positive than that at Au/MPA/PLL/HRP without the addition of graphene components (curve *b*). This might be attributed to the presence of graphene, which promotes electron transfer and endows electrocatalysis toward H_2O_2 at this graphene assembly biosensor as a result of its specific properties, such as high electrical conductivity and high specific surface area.[17]

The immobilization and bioactivity of HRP on a Au/MPA/graphene-PLL/HRP electrode was also examined by a standard procedure.[34] The Au/MPA/graphene-PLL/HRP electrode was immersed into 5.0 mL of stirred phosphate buffer solution containing 10 mM 4-aminophenazone, 80 mM phenol, and 1 mM H_2O_2. After a few minutes, the color of the solution turned red, and the UV−vis absorption spectra was collected in this step (as shown as the inset in Figure 4). The absorption peak at 505 nm indicated that the HRP on the Au/MPA/graphene-PLL/HRP electrode still had a similar physiological function for catalyzing the reduction of H_2O_2.

The chronoamperometric response of the Au/MPA/graphene-PLL/HRP electrode upon successively injecting H_2O_2 at a working potential of −0.3 V was performed (Figure S3). The Au/MPA/graphene-PLL/HRP electrode showed fast and good linear response from 0.5 mM to 10 mM (R = 0.998), and the Au/MPA/graphene-PLL/HRP electrode showed higher sensitivity (17.91 $\mu A \cdot mM^{-1} \cdot cm^{-2}$) than the Au/MPA/PLL/HRP modified electrode (5.59 $\mu A \cdot mM^{-1} \cdot cm^{-2}$).

(34) Schwartz, M. K. *Handbook of Enzymatic Methods of Analysis*; Dekker: New York, 1976.

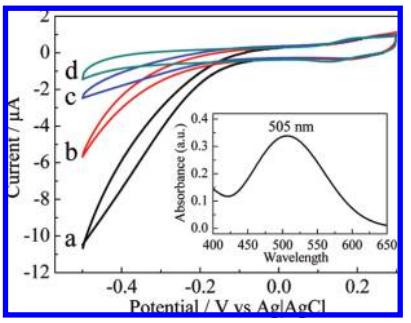

Figure 4. Cyclic voltammograms of (a) Au/MPA/graphene-PLL/HRP, (b) Au/MPA/PLL/HRP, (c) Au/MPA/graphene-PLL electrodes in phosphate buffer (0.05 M, pH 7.4) containing 5 mM H_2O_2, and (d) Au/MPA/graphene-PLL/HRP in phosphate buffer. Scan rate: 50 mV/s. The inset is a UV−vis absorption spectrum of the Trinder reaction at a Au/MPA/graphene-PLL/HRP electrode.

Conclusion

In summary, novel PLL-functionalized graphene nanocomposites were synthesized, which are promising in biological applications. The PLL-functionalized graphene was very water-soluble and had a large number of free active amino groups. Additionally, here, graphene sheets played an important role as connectors to assemble these amino groups, which offered a biocompatible and relatively friendly environment for further immobilization of biomolecules. As a potential application, HRP has been modified successfully on these graphene-PLL nanocomposites, and the resulting biosensor based on such graphene-PLL/HRP composites exhibited amplified biosensing toward H_2O_2.

Acknowledgment. This work was financially supported by the NSFC, China (No. 20673109) and the Ministry of Science and Technology (Nos. 2007AA03Z354 and 2007BAK26B06).

Supporting Information Available: XPS spectra, energy dispersive X-ray spectra, and chronoamperometric curves. This material is available free of charge via the Internet at http://pubs.acs.org.